

PAPER • OPEN ACCESS

The $^{46}\text{Ar}(^3\text{He}, d)^{47}\text{K}$ direct reaction as a probe of the ^{46}Ar proton wavefunction

To cite this article: D Brugnara *et al* 2023 *J. Phys.: Conf. Ser.* **2586** 012073

View the [article online](#) for updates and enhancements.

You may also like

- [RIPTIDE: a novel recoil-proton track imaging detector for fast neutrons](#)
A. Musumarra, F. Leone, C. Massimi et al.
- [A facility to validate photomultipliers for the upgrade of the Pierre Auger Observatory.](#)
M. Buscemi, M. Aglietta, F.C.T. Barbato et al.
- [Assembly and test of prototype scintillator tiles for the plastic scintillator detector of the High Energy Cosmic Radiation Detection \(HERD\) facility](#)
C. Altomare, F. Alemanno, F.C.T. Barbato et al.

PRIME
PACIFIC RIM MEETING
ON ELECTROCHEMICAL
AND SOLID STATE SCIENCE

HONOLULU, HI
Oct 6–11, 2024

Abstract submission deadline:
April 12, 2024

Learn more and submit!

Joint Meeting of
The Electrochemical Society
•
The Electrochemical Society of Japan
•
Korea Electrochemical Society

The $^{46}\text{Ar}(^3\text{He},d)^{47}\text{K}$ direct reaction as a probe of the ^{46}Ar proton wavefunction

D Brugnara¹, A Gottardo¹, M Assié², D Mengoni^{3,4}, A Lemasson⁵, E Clement⁵, F Flavigny⁶, D Ramos⁵, F Galtarossa², A Matta⁶, V Girard-Alcindor², M Babo², D Bazzacco³, D Beaumel², Y Blumenfeld², S Bottoni⁷, U Datta⁸, G de Angelis¹, G de France⁵, J Dudouet⁹, J Duenas¹⁰, A Goasduff¹, E T Gregor¹, F Hammache², A Illana¹, L Lalanne², S Leblond¹¹, I Lombardo¹², N Marchini¹³, B Million⁷, F Recchia⁴, K Rezynkina^{3,4}, M Rocchini¹³, J S Rojo¹⁴, M Siciliano¹¹, J J Valiente-Dobón¹, I Zanon¹, M Zielinska¹¹

¹Istituto Nazionale di Fisica Nucleare (INFN), Laboratori Nazionali di Legnaro, Legnaro, Italy

²IJClab, Université Paris Saclay, CNRS, Orsay, France

³Istituto Nazionale di Fisica Nucleare (INFN), Sezione di Padova, Padova, Italy

⁴Dipartimento di Fisica, Università degli Studi di Padova, Padova, Italy

⁵Grand Accélérateur National d'Ions Lourds (GANIL), Caen, France

⁶LPC Caen, Caen, France

⁷Istituto Nazionale di Fisica Nucleare (INFN), Sezione di Milano, Milano, Italy

⁸Saha Institute of Nuclear Physics, Kolkata, India

⁹Université de Lyon, CNRS/IN2P3, Villeurbanne Cedex, France

¹⁰Universidad de Huelva, Huelva, Spain

¹¹CEA Saclay, Université Paris-Saclay, Gif-sur-Yvette, France

¹²Istituto Nazionale di Fisica Nucleare (INFN), Sezione di Catania, Catania, Italy

¹³Istituto Nazionale di Fisica Nucleare (INFN), Sezione di Firenze, Firenze, Italy

¹⁴TRIUMF, Vancouver, British Columbia, Canada

Abstract. The discrepancy between shell-model calculations and intermediate-energy Coulomb excitation measurements in ^{46}Ar still stands as an unsolved puzzle in understanding the $N = 28$ shell evolution. This phenomenon has significant relevance considering the remarkable achievements of the shell model and the SDPF-U interaction in the region which is able to predict the fading of the $N = 28$ shell gap in neutron-rich ^{44}S . Recent measurements narrowed down this discrepancy to an overestimation of the proton amplitude to the quadrupole transition matrix element. The current work aims to propose a different perspective on the puzzle, by studying a direct proton-transfer reaction on ^{46}Ar as a means to directly probe the proton wavefunction of the ground state of this isotope. By measuring the amount of $l = 0$ transfer to the ground state ($1/2^+$) of ^{47}K with respect to the $l = 2$ to the first excited state ($3/2^+$), we aim to gain insight into the ground state proton wavefunction of ^{46}Ar . We will present a brief description of the experiment performed at the SPIRAL1 facility in GANIL (France). The experimental apparatus allowed a full reconstruction of the two-body reaction thanks to the combination of AGATA, VAMOS, MUGAST, CATS2, and HECTOR.



1. Introduction

The shell evolution along the neutron-rich $N = 28$ shell closure has been the subject of a multitude of experimental and theoretical studies [1]. The prediction of the fading of this shell gap below $Z = 16$ marks one of the outstanding achievements of the shell model and the SDPF-U interaction. ^{46}Ar , located just below the doubly magic nucleus ^{48}Ca lies in a region of transition

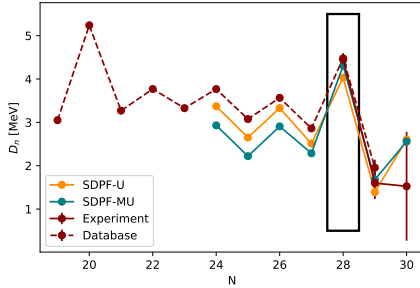


Figure 1. Trend of the D_n parameter (related to the neutron separation energy) in the ^{46}Ar isotopic chain. Data present in literature and adapted from [5] and extended with [6].

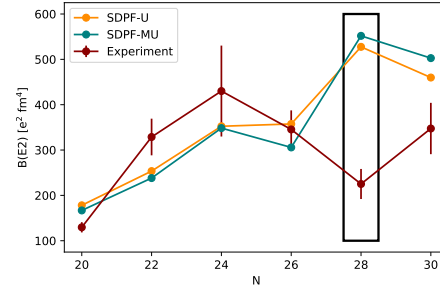


Figure 2. Transition probability $b_{\uparrow}(e2)$ between the 0^+ (g.s.) and the 2^+ (first excited state) in the Ar isotopic chain. Comparison of experimental data and calculations adapted from reference [8].

between ground states dominated by spherical configurations and the onset of collectivity found in the deformed ground state of ^{44}S . Experimental data obtained by neutron-knockout [2] and (d,p) reactions [3, 4], signals the persistence of a gap which is partially eroded by the onset of collectivity. Nevertheless, separation energies (S_n) offer a unique insight into the evolution of the shell gap across a shell closure. Recent measurements [5] allowed to observe the evolution of the parameter $D_n(Z, A) = (-1)^{N+1} [S_n(Z, A+1) - S_n(Z, A)]$, which relates separation energies of nearby isotopes, in the argon isotopic chain (Figure 1). The odd-even staggered trend with a significant increase for $N = 28$ further corroborates the picture painted by previous experiments. The remarkable agreement with shell-model calculations would indicate a good understanding of the shell evolution in ^{46}Ar . The striking discrepancy between the same shell-model calculations and multiple intermediate-energy Coulomb excitation experiments [4, 7, 8], aimed at measuring the transition probability between the g.s. (0^+) and the first excited state (2^+) of ^{46}Ar , has puzzled the community. Figure 2 shows the evolution of transition probabilities along the isotopic chain ($B_{\uparrow}(E2; 0^+ \rightarrow 2^+)$). In correspondence to the shell closure, the experimental data indicates a drop in probability, at odds with the shell-model prediction which shows the maximum value in ^{46}Ar . At the same time, calculations reproduce a similar trend for the remaining isotopes in the chain. The transition probability of a closed neutron shell isotope is inherently dependent on the proton component of the wave function. This reveals a duality between observables which are mostly affected by the neutron or the proton wave function. The former are well reproduced by shell-model calculations while the latter are incompatible specifically in ^{46}Ar . This hypothesis is confirmed by the authors of reference [4] which exploits the (p,p') reaction to assess the proton and neutron contribution to the total quadrupole matrix element. The comparison with shell-model calculations indicates an overestimation of the proton amplitude when compared to the experimental data.

2. The proton-transfer experiment

Direct reactions offer the unique possibility to probe directly the proton component of the g.s. wave function of ^{46}Ar . The shell model describes the 0^+ g.s. of ^{46}Ar as the equiprobable

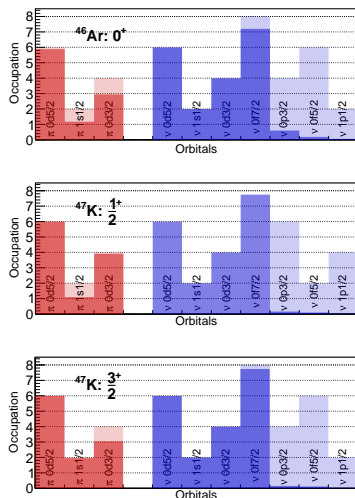


Figure 3. Occupation of the various valence orbitals for protons (in red) and neutrons (in blue) as a result of shell-model calculations with the SDPF-U interaction. ^{46}Ar (top panel) is described as two holes in ^{48}Ca , with comparable probabilities of finding the proton pair in the $s_{1/2}$ and $d_{3/2}$ orbitals. The g.s. of ^{47}K (middle panel), on the other hand, is a hole state in the $s_{1/2}$. Conversely, the $3/2^+$ state is a hole in the $d_{3/2}$. This picture of ^{47}K is supported by spectroscopic factors assessed from the $^{48}\text{Ca}(\vec{d}, ^3\text{He})^{47}\text{K}$ reaction [9].

combination of two proton pairs in the $s_{1/2}$ or in the $d_{3/2}$ (Figure 3). This is correlated to the prediction of almost degenerate $s_{1/2}$ and $d_{3/2}$ effective single-particle orbitals. On the other hand, the first two states of ^{47}K are well understood in terms of single-particle hole states in ^{48}Ca . The $1/2^+$ g.s. ($3/2^+$ excited state) is understood as a hole in the $s_{1/2}$ ($d_{3/2}$). Experimentally this picture is supported by the clear results obtained from the proton-removal direct reaction on ^{48}Ca : $^{48}\text{Ca}(\vec{d}, ^3\text{He})^{47}\text{K}$ [9]. The authors identify a total of two $j = 1/2^+$ ($j = 3/2^+$) states populated by means of $l = 0$ ($l = 2$) transfer. In both cases, the sum rule of the inferred spectroscopic factors, exhausted the shell-model limit, indicating little fragmentation of the single particle strength. In both cases, most of the spectroscopic amplitude is concentrated in the ground state $1/2^+$ and the first excited $3/2^+$ state, which are the subject of the current study. As a consequence, the probability of populating these single-particle states of ^{47}K with



Figure 4. Heuristic picture of the proton-transfer direct reaction. The probability of transferring a proton with $l = 0$ ($l = 2$) angular momentum to the $1/2^+$ ($3/2^+$) state of ^{47}K is linked to the ground state properties of ^{46}Ar . In the shell model picture, it is related to the occupation of the effective single particle orbitals of the 0^+ state.

a proton-transfer direct reaction is directly linked to the occupancy of the two valence orbitals in the argon isotope (Figure 4).

3. The experimental setup

The completeness of the experimental setup played a key role in the reconstruction of the reaction, providing detection and identification of the heavy and light fragments. The radioactive ^{46}Ar beam provided by the SPIRAL1 facility in GANIL (France) with an rate of ≈ 40 kHz impinged on a ^3He cryogenic target [10], HECTOR. Figure 5 shows the extent of the apparatus. The VAMOS++ magnetic spectrometer [11], in zero-degree configuration, tagged the ^{47}K

fragments while also accepting the beam for monitoring purposes. The detection of the heavy ions allowed a Doppler correction on an event-by-event basis. The deuterons were detected at backward angles by a double sided silicon strip detector, MUGAST [12], and identified by correlating the energy and the time of flight of each detected particle. The AGATA high-purity germanium tracking array [13] allowed the detection of gamma rays emitted by the decay of excited states of ^{47}K . The beam tracker, CATS2 [14], was used to monitor the beam spot 2 m before the target position and provided the timing information for MUGAST and VAMOS. The analysis of the experiment relies upon the measurement of the angular distribution of the

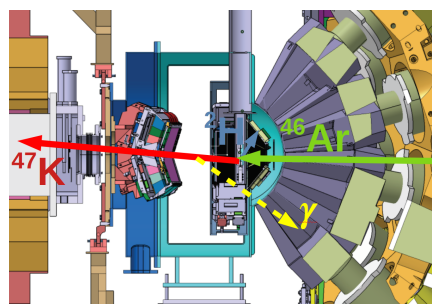


Figure 5. The extent of the experimental setup which comprises a magnetic spectrometer, VAMOS, a double sided silicon strip detector, MUGAST, and a high-purity germanium tracking array, AGATA. The cryogenic ^3He target, HECTOR, reached a constant temperature of 7 K throughout the experiment.

deuteron at backward angles. The amount of $l = 0$ and $l = 2$ transfer is extrapolated by means of a maximum likelihood maximization based on Monte Carlo Geant4 simulations of the experimental apparatus. This is necessary due to the little separation in excitation energy (360 keV) between the ground state and the first excited state of ^{47}K that cannot be resolved experimentally. Nevertheless, the $l = 0$ transfer, peaked at small angles in the center of mass (backward angles in the laboratory), has a strong angular distribution signature in comparison with the $l = 2$. In the course of the experiment, also the $l = 3$ transfer to the $7/2^-$ state was observed, consistent with the empty $f_{7/2}$ proton orbital. The result of the analysis will allow us to compare the relative spectroscopic factor inferred from the exclusive cross sections with theoretical calculations.

4. Conclusions

The aim of the experiment here introduced is to approach the transition probability problem in ^{46}Ar by studying directly the proton wavefunction of the ground state of this isotope with a proton transfer reaction. This, in turn, will help to shed light on the nature of the ground state of this isotope by comparison with state-of-the-art shell-model calculations.

References

- [1] Sorlin O and Porquet M-G 2013 *Phys. Scr.* **T152** 014003
- [2] Gade A *et al* 2005 *Phys. Rev. C* **71** 051301
- [3] Gaodefroy L *et al* 2008 *Phys. Rev. C* **78** 034307
- [4] Scheit H *et al* 1996 *Phys. Rev. Lett.* **77** 3967
- [5] Meisel Z *et al* 2015 *Phys. Rev. Lett.* **114** 022501
- [6] JAEA Nuclear Data Center Accessed: 26-10-2022 <https://www.ndc.jaea.go.jp/cgi-bin/nucltab14?18>
- [7] Gade A *et al* 2003 *Phys. Rev. C* **68** 014302
- [8] Calinescu S *et al* 2016 *Phys. Rev. C* **93** 044333
- [9] Banks S M *et al* 1985 *Nucl. Phys. A* **437** 381
- [10] Galtarossa F *et al* 2021 *Nucl. Instrum. Methods Phys. Res., Sect. A* **1018** 165830
- [11] Rejmund M *et al* 2021 *Nucl. Instrum. Methods Phys. Res., Sect. A* **646** 1684
- [12] Assié M *et al* 2021 *Nucl. Instrum. Methods Phys. Res., Sect. A* **1014** 165743
- [13] Akkoyun S *et al* 2012 *Nucl. Instrum. Methods Phys. Res., Sect. A* **668** 26
- [14] Ottini-Hustache S *et al* 1999 *Nucl. Instrum. Methods Phys. Res., Sect. A* **431** 476